

Supplementary Material: Stereodynamic control of cold rotationally inelastic CO + HD collisions

Pablo G. Jambrina,¹ James F. E. Croft,^{2,3} Naduvalath Balakrishnan,⁴ and F.J. Aoiz⁵

¹*Departamento de Química Física. University of Salamanca, Salamanca, 37008, Spain. e-mail: pjambrina@usal.es*

²*Department of Physics, University of Otago, Dunedin 9054, New Zealand. e-mail: j.croft@otago.ac.nz*

³*Dodd-Walls Centre for Photonic and Quantum Technologies, Dunedin 9054, New Zealand.*

⁴*Department of Chemistry and Biochemistry, University of Nevada, Las Vegas, NV 89154, USA. e-mail: naduvala@unlv.nevada.edu*

⁵*Departamento de Química Física. Universidad Complutense. Madrid 28040, Spain. e-mail:aoiz@quim.ucm.es*

I. CONVERGENCE DETAILS

Scattering calculations were performed in full-dimensionality using a modified version of the TwoBC code¹ following the approach described in Refs. 2–4, as it is described in the main text. The Potential Energy Surface (PES) used was the recent high-accuracy 6D CO-H₂ potential by Faure et al.^{5,6}

The coupled channel equations were propagated from 2 to 92 a_0 with a radial step size of $1.25 \times 10^{-1} a_0$. The number of points in the radial coordinate for each dimer for the discrete variable representation was 18; the number of points in the angular coordinate θ between \vec{R} and \vec{r} for each dimer for the Chebyshev quadrature was 12; the number of points in the dihedral angle between θ_1 and θ_2 for the Gauss-Hermite quadrature was 8. The basis set for the CO dimer included vibrational levels 0 and 1 with rotational levels up to 8 and 2 respectively, while for HD rotational levels up to 4 were included. Scattering calculations were performed for $J \leq 12$.

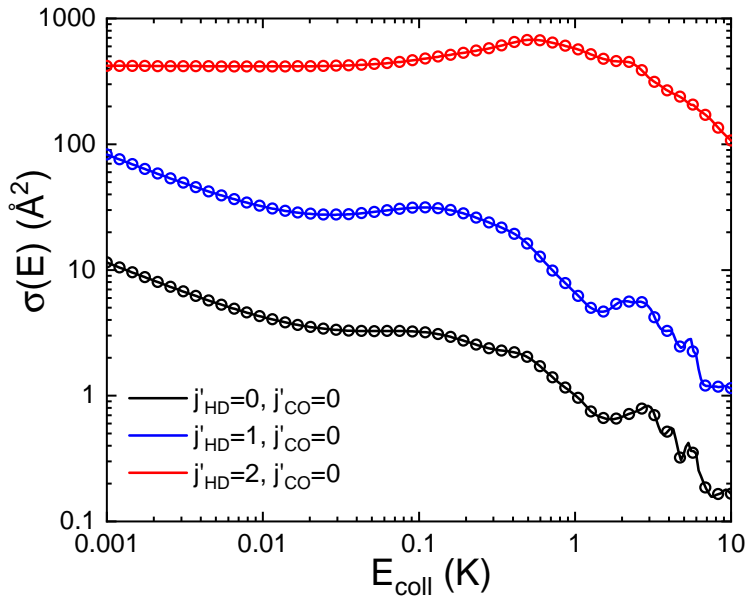


Fig S 1. Comparison of the production basis set with an expanded basis to check convergence. Integral cross sections for the HD($j_{\text{HD}}=2$) + CO($j_{\text{CO}}=0$) \rightarrow HD($j'_{\text{HD}}=0-2$) + CO($j'_{\text{CO}}=0$) transitions are shown, the solid lines correspond to the production basis set while the circles correspond to the expanded basis. It can be seen that no difference is observed at the scale shown and the low energy behaviour is correctly reproduced.

To check convergence with respect to the basis set and radial propagation the integral cross section was computed for the $20 \rightarrow 00$, 10 , and 20 transitions with $J \leq 5$ using an expanded basis: λ_1 was restricted to $0-10$ while λ_2 was restricted to $0-6$; The coupled channel equations were propagated from 1.5 to $102 a_0$ with a radial step size of $1.05 \times 10^{-1} a_0$; The basis set for the CO dimer included vibrational levels 0 and 1 with rotational levels up to 10 and 4 respectively, while for HD only the ground vibrational level was included with rotational levels up to 6 . Fig. S1 compares the integral cross-sections computed using both basis sets. The solid lines correspond to the “production” basis set described in the previous paragraph while the black crosses on a course grid correspond to the expanded basis, it can be seen that no difference is observed at the scale shown and the low energy behaviour is correctly reproduced.

II. NATURE OF THE RESONANCE

To identify the origin of the observed resonance peak at 0.1 K depicted in Fig. 1 of the main text, we analyzed the effective potentials corresponding to different incoming partial waves L ,

$$V^J(R) = \epsilon_{j_1 j_2} + U_{j_1 j_2 L j_{12}, j'_1 j'_2 L' j'_{12}}(R) + \frac{L(L+1)\hbar^2}{2\mu R^2}. \quad (1)$$

where $\epsilon_{j_1 j_2}$ is the energy of the combined molecular state obtained by adding the asymptotic rovibrational energies of HD and CO. $U_{j_1 j_2 L j_{12}, j'_1 j'_2 L' j'_{12}}(R)$ is the diabatic potential energy coupling matrix, and the third term is the centrifugal potential for the orbital angular momentum L . Following the procedure described in Ref. 7, the diabatic potential energy coupling matrix is diagonalized at each intermolecular separation (R), with the eigenvalues corresponding to the adiabatic potentials.

Fig. S2 shows the diagonal diabatic potentials corresponding to the incoming channel with HD($j = 2$) and CO($j = 0$). The heights of the centrifugal barriers for $L = 1, 2, 3$, and 4 are $0.06, 0.31, 0.87$, and 1.82 K respectively. Fig. S3 shows the elastic cross section computed by separately solving the radial Schrödinger equation on each of the diabatic potentials corresponding to $0 < L \leq 4$. It can clearly be seen that in the $L = 2$ channel there is a shape resonance at around 0.1 K. In Fig. 2 of the main text, it is shown that there is also a significant contribution of $L=1$ scattering at the 0.1 K resonance. Since the centrifugal barrier for $L=1$ is just 0.06 K, $L=1$ contribution seems to be originated by an

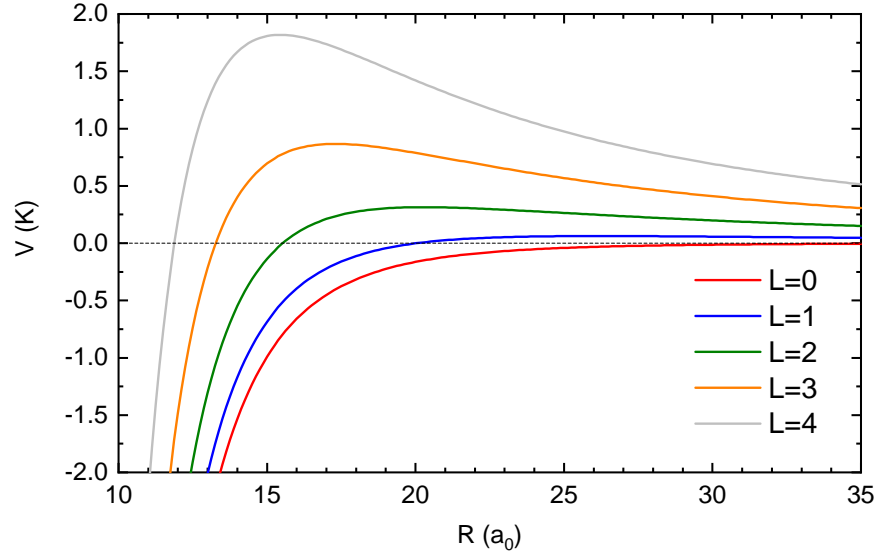


Fig S 2. One dimensional diabatic potentials as a function of R for the incoming channel with $\text{HD}(j = 2)$ and $\text{CO}(j = 0)$.

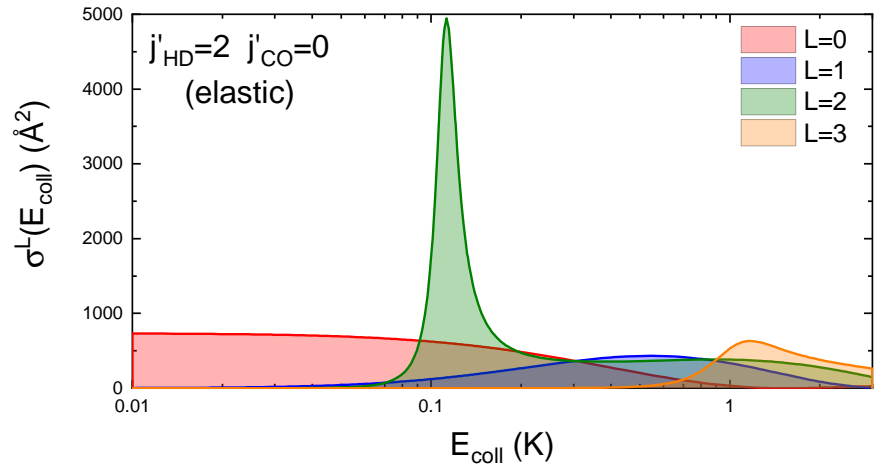


Fig S 3. Elastic cross section corresponding to the diabatic potentials shown in Fig. S2.

“above-the-barrier” resonance.

REFERENCES

¹R. Krems, TwoBC – quantum scattering program, University of British Columbia, Vancouver, Canada, 2006.

²G. Quémener, N. Balakrishnan and R. V. Krems, *Phys. Rev. A*, 2008, **77**, 030704.

- ³G. Quéméner and N. Balakrishnan, *J. Chem. Phys.*, 2009, **130**, 114303.
- ⁴S. F. dos Santos, N. Balakrishnan, S. Lepp, G. Quéméner, R. C. Forrey, R. J. Hinde and P. C. Stancil, *J. Chem. Phys.*, 2011, **134**, 214303.
- ⁵A. Faure, P. Jankowski, T. Stoecklin and K. Szalewicz, *Sci. Rep.*, 2016, **6**, 28449.
- ⁶G. Garberoglio, P. Jankowski, K. Szalewicz and A. H. Harvey, *J. Chem. Phys.*, 2017, **146**, 054304.
- ⁷J. F. E. Croft, N. Balakrishnan, M. Huang and H. Guo, *Phys. Rev. Lett.*, 2018, **121**, 113401.